SCIENTIFIC REPORTS

OPEN

SUBJECT AREAS:
SUPERCONDUCTING PROPERTIES AND MATERIALS
ELECTRONIC PROPERTIES AND MATERIALS

Received
24 April 2014

Accepted
14 November 2014

Published
3 December 2014

Correspondence and requests for materials should be addressed to T.Y. (yoshida.teppei.8v@kyoto-u.ac.jp)

* Current address: Graduate School of Human and Environmental Studies, Kyoto University, Yoshida-nohonmatsu-cho, Sakyo-ku, Kyoto 606-8501, Japan.

† Current address: Department of Advanced Materials Science, University of Tokyo, Kashiwa 277-8561, Japan.

Anisotropy of the superconducting gap in the iron-based superconductor $BaFe_2(As_{1-x}P_x)_2$

T. Yoshida[1,2]*, S. Ideta[1], T. Shimojima[3], W. Malaeb[4], K. Shinada[3], H. Suzuki[1], I. Nishi[1], A. Fujimori[1,2], K. Ishizaka[3], S. Shin[4], Y. Nakashima[5], H. Anzai[6], M. Arita[6], A. Ino[5], H. Namatame[6], M. Taniguchi[5,6], H. Kumigashira[7], K. Ono[7], S. Kasahara[8,9], T. Shibauchi[9]†, T. Terashima[8], Y. Matsuda[9], M. Nakajima[1], S. Uchida[1,2], Y. Tomioka[2,10], T. Ito[2,10], K. Kihou[2,10], C. H. Lee[2,10], A. Iyo[2,10], H. Eisaki[2,10], H. Ikeda[2,9], R. Arita[2,3], T. Saito[2,11], S. Onari[2,12] & H. Kontani[2,11]

[1]Department of Physics, University of Tokyo, Bunkyo-ku, Tokyo 113-0033, Japan, [2]JST, Transformative Research-Project on Iron Pnictides (TRIP), Chiyoda, Tokyo 102-0075, Japan, [3]Department of Applied Physics, University of Tokyo, Tokyo 113-8656, Japan, [4]Institute of Solid State Physics, University of Tokyo, Kashiwa 277-8581, Japan, [5]Graduate School of Science, Hiroshima University, Higashi-Hiroshima 739-8526, Japan, [6]Hiroshima Synchrotron Radiation Center, Hiroshima University, Higashi-Hiroshima 739-0046, Japan, [7]KEK, Photon Factory, Tsukuba, Ibaraki 305-0801, Japan, [8]Research Center for Low Temperature and Materials Sciences, Kyoto University, Kyoto 606-8502, Japan, [9]Department of Physics, Kyoto University, Kyoto 606-8502, Japan, [10]National Institute of Advanced Industrial Science and Technology (AIST), Tsukuba 305-8568, Japan, [11]Department of Physics, Nagoya University, Furo-cho, Nagoya 464-8602, Japan, [12]Department of Applied Physics, Nagoya University, Furo-cho, Nagoya 464-8602, Japan.

We report peculiar momentum-dependent anisotropy in the superconducting gap observed by angle-resolved photoemission spectroscopy in $BaFe_2(As_{1-x}P_x)_2$ ($x = 0.30$, $T_c = 30$ K). Strongly anisotropic gap has been found only in the electron Fermi surface while the gap on the entire hole Fermi surfaces are nearly isotropic. These results are inconsistent with horizontal nodes but are consistent with modified $s_{\pm}$ gap with nodal loops. We have shown that the complicated gap modulation can be theoretically reproduced by considering both spin and orbital fluctuations.

In the iron-based superconductors, most of the experimental studies have so far indicated that the superconducting (SC) gap is nodeless and opens on all Fermi surfaces (FSs) in contrast to the *d*-wave SC gap of the high-T_c cuprate superconductors[1]. However, it is unclear whether the SC order parameter is a conventional *s* wave without sign change (s_{++} wave) or its sign changes between FSs ($s_{\pm}$ wave). According to theories of spin-fluctuation-mediated superconductivity, various SC gap structures, such as nodeless $s_{\pm}$-wave, nodal *s*-wave, and nodal *d*-wave, are realized depending on the FS geometry[2–4]. On the other hand, observation of orbital-polarized states[5] and the strong softening of the shear modulus C_{66}[6,7] stimulate theoretical studies of the orbital-fluctuation-mediated superconductivity, which favor the s_{++} state without sign change[8–10].

In contrast to the full-gap superconductivity in most of the iron-based superconductors, some systems show signatures of line nodes in the SC gap. While most of the nodal SC compounds such as KFe_2As_2[11,12] show low $T_c <$ 10 K, $BaFe_2(As_{1-x}P_x)_2$[13–15] has a relatively high T_c (~30 K) and is a suitable system for this purpose. In an angle-resolved thermal conductivity measurement[16], four-fold symmetry as a function of magnetic field direction has been observed in the vortex state, suggestive of loop-like line nodes on the electron FS[17,18].

Angle-resolved photoemission spectroscopy (ARPES) is the most direct and powerful technique to unambiguously determine the location of line nodes in momentum space. For example, "octet line nodes" in KFe_2As_2 has been recently reported[12]. In $BaFe_2(As_{1-x}P_x)_2$, laser ARPES studies[19,20] have revealed nearly isotropic and FS-independent superconducting gaps on the hole FSs around the *Z* point, indicating the importance of orbital fluctuations in the pairing mechanism[8–10]. However, in a recent study using synchrotron radiation by Zhang *et al.*[21], a "horizontal line node"[22,23] has been observed on the outer hole FS around the *Z* point. Because no in-plane anisotropy was found in both ARPES results[19,21], the fourfold symmetry of the thermal conductivity[16] remains to be explained.

In this study, in order to resolve this controversy, we have performed an ARPES study of $BaFe_2(As_{1-x}P_x)_2$ and clarified that there is no horizontal node on the hole FSs and the SC gaps are isotropic for all k_z's, consistent with

the laser ARPES study[19,20]. Furthermore, we have revealed that gap nodes or at least strong anisotropy exists on the inner electron FS, which enables us to understand the fourfold symmetry in the thermal conductivity[16]. We have shown that a theoretical model including not only spin fluctuations but also orbital fluctuations well reproduces the observed SC gap structure, suggestive of a pairing mechanism beyond spin fluctuations.

Results

Energy gaps of the hole Fermi surfaces. Energy gaps of the hole FSs for $BaFe_2(As_{1-x}P_x)_2$ ($x = 0.30$, $T_c = 30$ K) around the Z point[20,21] are presented in Fig. 1. We observed at least two hole dispersions, implying that two out of the three bands are nearly degenerated as in the previous studies[19,21,24]. The spectra at $T = 15$ K show a dip at E_F for both bands, indicating a clear gap opening. The temperature dependence of the energy distribution curves (EDCs) at the Fermi momentum k_F [Figs. 1(c1), 1(c2)] shows a clear gap opening even slightly above T_c, unlike the previous result[21].

We have also investigated the gap anisotropy of the hole FSs [Fig. 1(e)]. In Figs. 1(d1)–1(d3), we show an example of the EDC at k_F below and above T_c. The symmetrized EDC below T_c have been divided by those above T_c and we obtain peak structure at ~6 meV [Fig. 1(d3)]. Since this structure evolves at low temperature as a shoulder in the EDCs [Fig. 1(d1)], we attributed this peak to a SC peak. Similar shoulders are observed at various k_F points on the outer hole FS [Fig. 1(e)] and their energies are nearly isotropic, consistent with the laser ARPES result[19]. Thus, the four-fold oscillation in the angle-resolved thermal conductivity measurements[16] is hardly explained by the isotropic character of the outer hole band.

Next, we present ARPES spectra of the hole FSs with various photon energies and hence for various k_z's as shown in Fig. 2. The photon energies $h\nu \sim 23$ eV and ~35 eV correspond to the k_z of the Γ and Z points, respectively [Fig. 2(d)]. Three hole dispersions are clearly resolved near the Γ point [Fig. 2(e)]. For the β and γ FSs [Figs. 2(b) and 2(c)], the gap energies are ~5–8 meV and are nearly independent of photon energy, i.e., independent of k_z. For the α and β bands [Figs. 2(a) and 2(b)], the EDCs around the Z point (~35 eV)

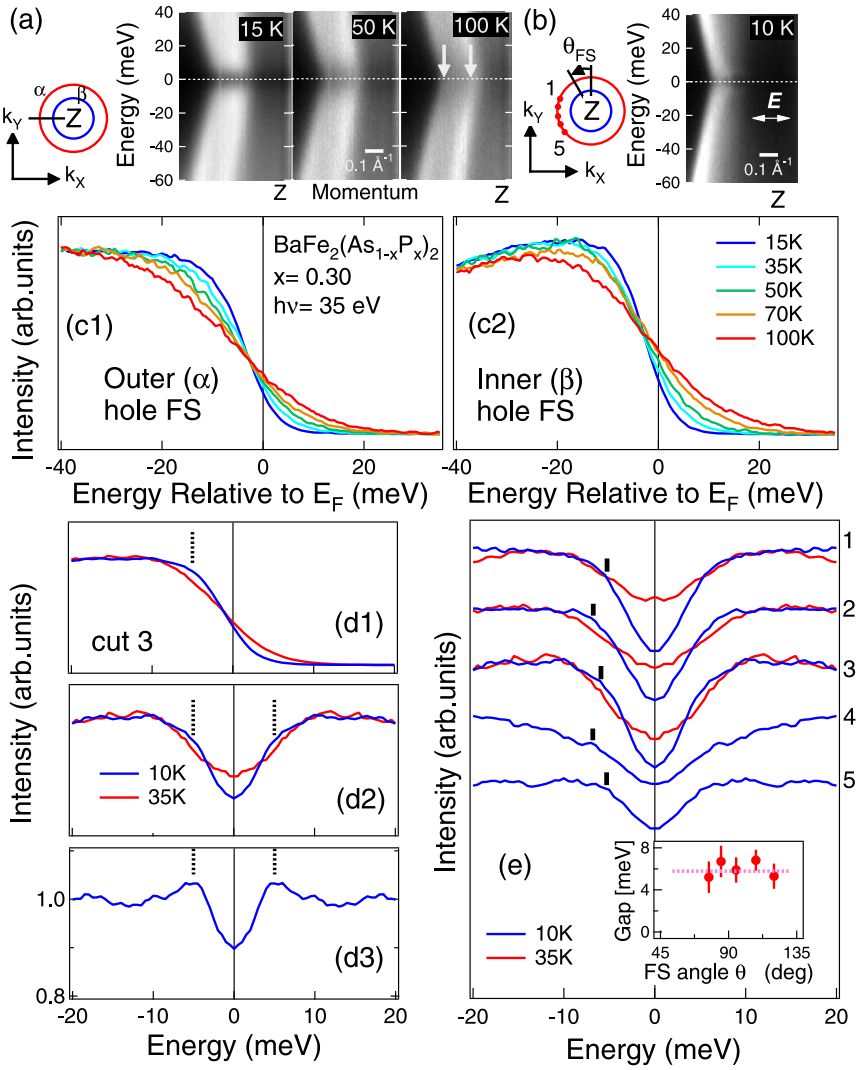

Figure 1 | Superconducting gap observed on the hole FSs in $BaFe_2(As_{1-x}P_x)_2$ ($x = 0.30$, $T_c = 30$ K) around the Z point ($h\nu = 35$ eV). (a) Temperature dependence of the symmetrized ARPES spectra in the k_X direction taken with a circularly polarized light. Fermi momentum k_F's are indicated by arrows in the data taken at $T = 100$ K. (b) Symmetrized ARPES spectra in the k_X direction (cut 3) with a linearly polarized light. The intensity of the outer hole band is enhanced due to matrix-element effect. (c1,c2) EDCs at k_F for the outer and inner hole FSs. (d1)-(d3) Temperature dependence of the EDC at k_F above and below T_c for cut 3 in panel (b). The EDCs in panel (d1) are symmetrized in panel (d2). The spectrum in panel (d3) has been obtained by dividing the spectrum below T_c by that above T_c in panel (d2). (e) Symmetrized EDCs corresponding to the k_F points in panel (b). Vertical bars indicate shoulders in the low temperature spectra, indicating a superconducting gap. (Inset) Sizes of the gaps are plotted as a function of Fermi surface angle θ_{FS}.

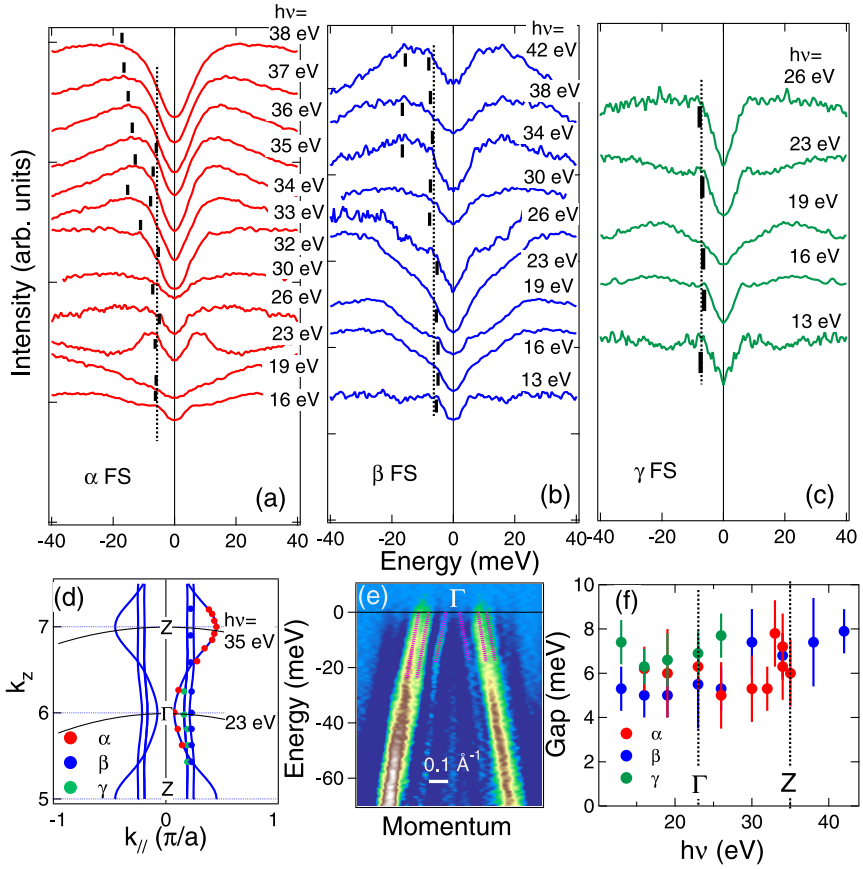

Figure 2 | Superconducting gap observed on the hole FSs with various k_z in $BaFe_2(As_{1-x}P_x)_2$ ($x = 0.30$, $T_c = 30$ K). (a–c) Symmetrized EDCs at k_F points in the Γ-X direction taken below T_c. Vertical bars indicate the gap energy. (d) Correspondence between the incident photon energy, k_z, and the three-dimensional hole FSs (blue curves). (e) Second derivative plots of the ARPES spectra around the Γ point. (f) Gaps estimated in panels a–c are plotted as a function of $h\nu$.

show a hump (at ~12–18 meV) with a shoulder (at ~7 meV). While the shoulder signifies a superconducting gap as in Fig. 1, the humps for the α and β FSs indicate a pseudogap[25,26]. The SC gap is nearly independent of $h\nu$ [panel (f)] and, hence, the hole FSs do not have an horizontal line node at any k_z.

Energy gaps of the electron Fermi surfaces. In order to investigate the possible existence of line nodes on the electron FSs, a photon energy of $h\nu = 40$ eV with a circularly polarized light was used as shown in Fig. 3, because with this polarization signals from the inner and outer electron FSs can be distinguished due to matrix element effects as shown in panel (a). In the inner electron FS [Fig. 3(b)], while the EDC at the Fermi surface angle $\theta_{FS} = 80^\circ$ shows a clear shift (~5 meV) from E_F, the shift of the EDC at $\theta_{FS} = 170^\circ$ is smaller (<~2 meV), indicating a strong anisotropy of the superconducting gap.

As in panel (b), the leading edge of the spectrum is useful to detect the gap anisotropy. Therefore, the crossing point between the EDCs below and above T_c [Figs. 3(c) and 3(d)] will reflect the magnitude of the SC gap. Also, we have determined the energy of SC peak in the same manner as in Fig. 1(d1)–(d3). In Figs. 3(e) and 3(f), the SC gap magnitudes estimated from the crossing point and the peak energy are plotted as a function of θ_{FS}. These plots indicate that the inner FS has a gap minimum near the edge of the FS ($\theta_{FS} \sim 0$ or 180°). We have also confirmed this strongly anisotropic SC gap for the inner electron FS with several experimental conditions. (See Supplementary Information, Figs. S2 and S3.) Although the minimum gap value in the inner FS appears to be finite, it should be remembered that ARPES has finite k_z resolution (inverse of the photoelectron mean-free-path ~0.5 nm). If the line nodes are distributed in a three dimensional shape such as a loop-like node[17,19,27], k_F's with finite gaps inevitably contribute to EDCs and the gap would look finite.

Discussion

Here, we illustrate a possible momentum dependence of the SC gap function from the present ARPES study in Fig. 4(a). The outer hole FS near the Z point does not show a signature of vertical nor horizontal line nodes. In contrast to the isotropic gap on the hole FSs, the gap minimum has been observed on the inner electron FS at the longer edge of the ellipsoid-shaped FS cross-section [Fig. 3 and Fig. 4]. Khodas and Chubukov[31] have shown the folded model of the electron pockets and deduced vertical loop-like nodes in the electron FSs. Even if this is the case, it is still difficult to reproduce the loop-like node if there are three hole FSs as in the present results[28]. Thus, the observed momentum dependence of the SC gap magnitude is difficult to understand from the spin-fluctuation-mediated mechanism alone. The comparable sizes of the SC gaps of the three hole FSs, that is, for FSs of different orbital character indicate that the inter-orbital scattering is required for the Cooper pair formation[8–10]. Also, the disappearance of the xy hole FS is required in the spin-fluctuation-mediated mechanism to achieve a strongly anisotropic gap or line nodes in the electron FSs[2,27], while we have clearly observed three hole bands including the xy hole FS around the Γ point (Fig. 2).

The three-dimensional gap structure in ref. 28 obtained by a model calculation including orbital fluctuations, shown in Fig. 4(b), shows common features with the experimental results of the hole and elec-

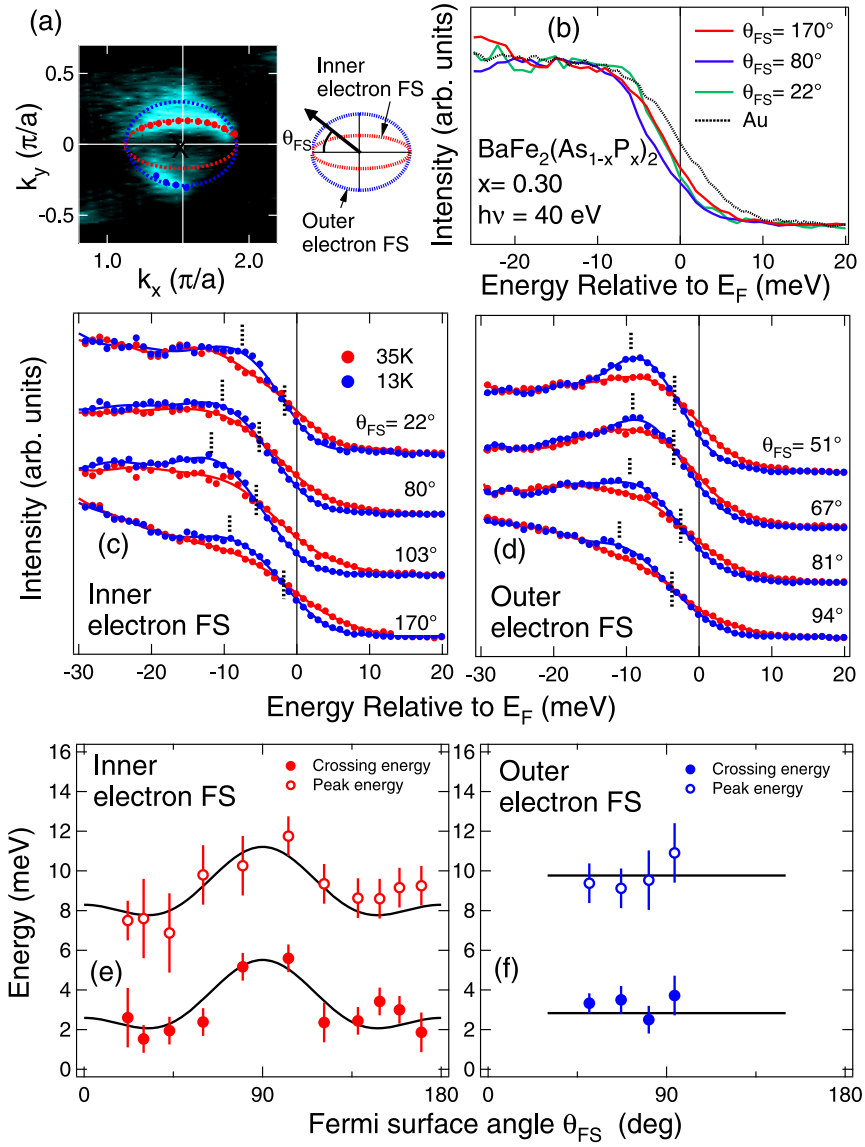

Figure 3 | Superconducting gap anisotropy observed on the electron FSs around the *X* point in $BaFe_2(As_{1-x}P_x)_2$ ($x = 0.30$, $T_c = 30$ K) taken at $h\nu = 40$ eV. (a) Fermi surface mapping using a circularly polarized light. The Fermi angle is defined so that the direction from *X* to Γ is $\theta_{FS} = 0$. (b) EDCs at k_F taken below T_c ($T = 13$ K) and compared with gold spectra. (c) (d) EDCs at k_F taken below ($T = 13$ K) and above ($T = 35$ K) T_c for the inner and outer FSs. Vertical bars indicate the peak positions and the crossing energy between the spectra below and above T_c. (e) (f) Energy of the peak and the crossing point for the inner and outer FSs are plotted as a function of Fermi surface angle θ_{FS}. While the SC gap of the inner FS is highly anisotropic, a clear anisotropy is not identified in the outer FS. We could not obtain the signal of the outer band near the edge of the FS because its intensity is weak and merges with the inner band.

tron FSs. In this model, when the inter-orbital scattering is moderately strong, the highly anisotropic gap of the electron FS is expected to have nodes in the crossover region between the $s_{\pm}$ and s_{++}-wave superconductivity. According to the calculated results[28], when a loop-like node appears at the longer edge of the electron FSs, a large part of the FS has an order parameter of opposite sign to that of the hole FSs. Thus, the present observation of the gap anisotropy in the electron FS indicates the realization of nearly $s_{\pm}$-wave SC state.

The present result on the SC gap of the hole FSs for the $x = 0.30$ sample described above have been qualitatively reproduced for a slightly overdoped $x = 0.38$ sample as shown in Supplementary Fig. S4 and, therefore, can be considered as robust features. Also, in the present study, while the two electron FSs have gap values ~8–10 meV, the hole FSs show relatively small values ~5–8 meV. This can be contrasted with the previous ARPES study of Ref. 21, which shows similar gap values between electron and hole FSs except around the Z point. Here, we discuss possible origins of the discrepancy in the SC gap anisotropy with the previous study by Zhang *et al.*[21]. We should note that the samples were grown by the self-flux method in our study while a flux-free method was applied in Ref. 21. In the process of the sample growth, starting compounds are different between these methods. Therefore, we speculate that such a difference in the sample growth may give differences in the local structure and/or unknown defects, hence, the detailed electronic structure.

In the present study, the strongly anisotropic SC gap and the absence of a horizontal node are suggestive of the mechanism beyond spin fluctuations such as orbital fluctuations. As a possible origin, inter-orbital interaction, electron-phonon interaction[8], and vertex correction of the Coulomb interaction[29] have been discussed so far. Since these interactions may depend on the doping level and material families, the pairing mechanism beyond spin fluctuations should be

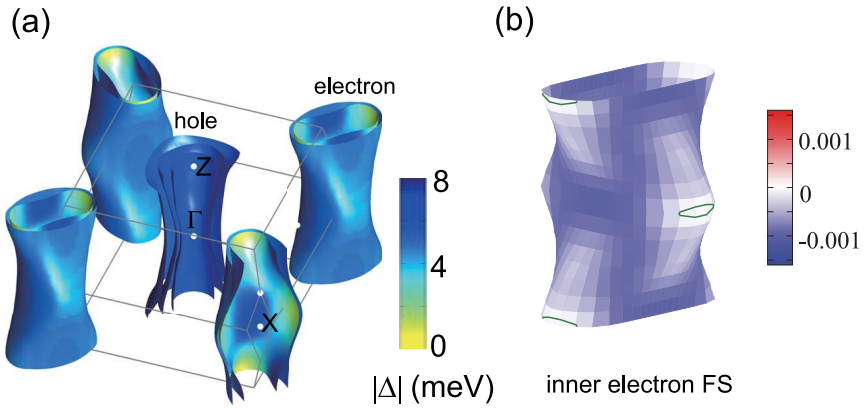

Figure 4 | SC gap Δ for the FSs of $BaFe_2(As_{1-x}P_x)_2$. (a) Momentum dependence of the Δ for $x = 0.30$ deduced from the present ARPES result. The color scale represents the magnitude of the SC gap. Loop-like nodes or gap minima appear near the rim of the inner electron FSs. (b) Theoretical calculation of the anisotropy for inner electron FS with orbital fluctuations in ref. 28. The green lines represent the gap nodes.

revealed in future systematic studies of the SC gap in various kinds of the iron pnictide superconductors.

Methods

Single crystals of $BaFe_2(As_{1-x}P_x)_2$ with $x = 0.30$ ($T_c = 30$ K) were grown by a self-flux method[30]. The details of the sample growth, characterization are described in Supplementary S1. ARPES experiments were carried out at BL 9A of Hiroshima Synchrotron Radiation Center (HiSOR) and BL-28A of Photon Factory (PF). At HiSOR BL 9A, a Scienta SES-R4000 analyzer and a circularly-polarized light were used with the total energy resolution of ~7–8 meV. At PF BL-28A, a Scienta SES-2002 analyzer and a circularly- and linearly-polarized light were used with the total energy resolution of ~8–10 meV. The crystals were cleaved *in situ* at $T = 8$–13 K in an ultra-high vacuum of $\sim 5 \times 10^{-11}$ Torr. Calibration of the Fermi level (E_F) of the samples was achieved by referring to that of gold. In-plane (k_x, k_y) and out-of-plane electron momenta (k_z) are expressed in units of π/a and $2\pi/c$, respectively, where $a = 3.92$ Å and $c = 12.8$ Å are the in-plane and the out-of-plane lattice constants. Here, the x and y axes point towards nearest neighbor Fe atoms. The correspondence between k_z and $h\nu$ has been determined in our previous ARPES studies[20,24].

1. Ding, H. *et al.* Observation of Fermi-surface–dependent nodeless superconducting gaps in $Ba_{0.6}K_{0.4}Fe_2As_2$. *Europhys. Lett.* **83**, 47001 (2008).
2. Kuroki, K. *et al.* Pnictogen height as a possible switch between high-T_c nodeless and low-T_c nodal pairings in the iron-based superconductors. *Phys. Rev. B* **79**, 224511 (2009).
3. Hirschfeld, P. J., Korshunov, M. M. & Mazin, I. I. *et al.* Gap symmetry and structure of Fe-based superconductors. *Rep. Prog. Phys.* **74**, 124508 (2011).
4. Chubukov, A. V. Pairing mechanism in Fe-based superconductors. *Annu. Rev. Condens. Matter Phys.* **3**, 57 (2012).
5. Shimojima, T. *et al.* Orbital-dependent modifications of electronic structure across the magnetostructural transition in $BaFe_2As_2$. *Phys. Rev. Lett.* **104**, 057002 (2010).
6. Yoshizawa, M. *et al.* Structural quantum criticality and superconductivity in iron-based superconductor $Ba(Fe_{1-x}Co_x)_2As_2$. *J. Phys. Soc. Jpn.* **81**, 024604 (2012).
7. Goto, T. *et al.* Quadrupole effects of layered iron pnictide superconductor $Ba(Fe_{0.9}Co_{0.1})_2As_2$. *J. Phys. Soc. Jpn.* **80**, 073702 (2011).
8. Kontani, H. & Onari, S. Orbital-fluctuation-mediated superconductivity in iron pnictides: analysis of the five-orbital Hubbard-Holstein model. *Phys. Rev. Lett.* **104**, 157001 (2010).
9. Saito, T., Onari, S. & Kontani, H. Orbital fluctuation theory in iron pnictides: Effects of As-Fe-As bond angle, isotope substitution, and Z2-orbital pocket on superconductivity. *Phys. Rev. B* **82**, 144510 (2010).
10. Zhang, J., Sknepnek, R., Fernandes, R. M. & Schmalian, J. Orbital coupling and superconductivity in the iron pnictides. *Phys. Rev. B* **79**, 220502 (2009).
11. Dong, J. K. *et al.* Quantum criticality and nodal superconductivity in the FeAs-based superconductor KFe_2As_2. *Phys. Rev. Lett.* **104**, 087005 (2010).
12. Okazaki, K. *et al.* Octet-line node structure of superconducting order parameter in KFe_2As_2. *Science* **337**, 1314 (2012).
13. Kasahara, S. *et al.* Evolution from non-Fermi- to Fermi-liquid transport via isovalent doping in $BaFe2(As_{1-x}P_x)_2$ superconductors. *Phys. Rev. B* **81**, 184519 (2010).
14. Hashimoto, K. *et al.* Line nodes in the energy gap of superconducting $BaFe_2(As_{1-x}P_x)_2$ single crystals as seen via penetration depth and thermal conductivity. *Phys. Rev. B* **81**, 220501 (2010).
15. Hashimoto, K. *et al.* A sharp peak of the zero-temperature penetration depth at optimal composition in $BaFe_2(As_{1-x}P_x)_2$. *Science* **336**, 1554 (2012).
16. Yamashita, M. *et al.* Nodal gap structure of superconducting $BaFe_2(As_{1-x}P_x)_2$ from angle-resolved thermal conductivity in a magnetic field. *Phys. Rev. B* **84**, 060507 (2011).
17. Mazin, I. I. *et al.* Pinpointing gap minima in $Ba(Fe_{0.94}Co_{0.06})_2As_2$ via band-structure calculations and electronic Raman scattering. *Phys. Rev. B* **82**, 180502 (2010).
18. Chubukov, A. V., Vavilov, M. G. & Vorontsov, A. B. Momentum dependence and nodes of the superconducting gap in the iron pnictides. *Phys. Rev. B* **80**, 140515 (2009).
19. Shimojima, T. *et al.* Orbital-independent superconducting gaps in iron pnictides. *Science* **332**, 564 (2011).
20. Shimojima, T. *et al.* Angle-resolved photoemission study on the superconducting iron-pnictides of $BaFe_2(As,P)_2$ with low energy photons. *Solid State Commun.* **152**, 695 (2012).
21. Zhang, Y. *et al.* Nodal superconducting-gap structure in ferropnictide superconductor $BaFe_2(As_{0.7}P_{0.3})_2$. *Nature Phys.* **8**, 371 (2012).
22. Suzuki, K., Usui, H. & Kuroki, K. Possible three-dimensional nodes in the $s_{\pm}$ superconducting Gap of $BaFe_2(As_{1-x}P_x)_2$. *J. Phys. Soc. Jpn.* **80**, 013710 (2011).
23. Graser, S. *et al.* Spin fluctuations and superconductivity in a three-dimensional tight-binding model for $BaFe_2As_2$. *Phys. Rev. B* **81**, 214503 (2010).
24. Yoshida, T. *et al.* Two-dimensional and three-dimensional Fermi surfaces of superconducting $BaFe_2(As_{1-x}P_x)_2$ and their nesting properties revealed by angle-resolved photoemission spectroscopy. *Phys. Rev. Lett.* **106**, 117001 (2011).
25. Kasahara, S. *et al.* Electronic nematicity above the structural and superconducting transition in $BaFe_2(As_{1-x}P_x)_2$. *Nature* **486**, 382 (2012).
26. Shimojima, T. *et al.* Pseudogap formation above the superconducting dome in iron pnictides *Phys. Rev. B* **89**, 045101 (2014).
27. Maiti, S. *et al.* Evolution of symmetry and structure of the gap in iron-based superconductors with doping and interactions. *Phys. Rev. B* **84**, 224505 (2011).
28. Saito, T., Onari, S. & Kontani, H. Nodal gap structure in Fe-based superconductors due to the competition between orbital and spin fluctuations. *Phys. Rev. B* **88**, 045115 (2013).
29. Onari, S. & Kontani, H. Self-consistent vertex correction analysis for iron-based superconductors: Mechanism of Coulomb-interaction-driven orbital fluctuations. *Phys. Rev. Lett.* **109**, 137001 (2012).
30. Nakajima, M. *et al.* Growth of $BaFe_2(As_{1-x}P_x)_2$ single crystals ($0 < x < 1$) by Ba_2As_3/Ba_2P_3-flux method. *J. Phys. Soc. Jpn.* **81**, 104710 (2012).
31. Khodas, M. & Chubukov, A. V. Vertical loop nodes in iron-based superconductors. *Phys. Rev. B* **86**, 144519 (2012).

Acknowledgments

We are grateful to K. Kuroki and D.L. Feng for enlightening discussions. This work was supported by a Grant-in-Aid for Scientific Research on Innovative Area "Materials Design through Computics: Complex Correlation and Non-Equilibrium Dynamics" from MEXT, the Japan-China-Korea A3 Foresight Program and a Grant-in-Aid for Young Scientist (B) (22740221) from the Japan Society for the Promotion of Science. ARPES experiments were carried out at HiSOR (Proposal No. 10-B-27 and 11-B-1) and Photon Factory (Proposal No. 2009S2-005, No. 2012S2-001, and No. 2012G075).

Author contributions

T.Y., S.I., T. Shimojima, W.M., K.S., H.S. and I.N. performed ARPES experiments. T.Y. and S.I. analyzed the ARPES data. S.K. and M.N. synthesized single crystals. K.I., S.S., Y.N., H.A., M.A., A.I., H.N., M.T., H. Kumigashira and K.O. supported synchrotron ARPES experiments. T. Shibauchi, T.T. and Y.M. supported growing single crystals at Kyoto University. S.U., Y.T., T.I., K.K., C.H.L., A.I. and H.E. supported growing single crystals at

AIST. H.I., R.A., T.S., S.O. and H. Kontani are responsible for theoretical part of the project. T.Y. and A.F. designed the project and wrote the manuscript with suggestions by T. Shibauchi, Y.M., S.U., H.I., R.A. and H. Kontani and all other coauthors.

Additional information

Supplementary information accompanies this paper at http://www.nature.com/scientificreports

Competing financial interests: The authors declare no competing financial interests.

How to cite this article: Yoshida, T. *et al.* Anisotropy of the superconducting gap in the iron-based superconductor $BaFe_2(As_{1-x}P_x)_2$. *Sci. Rep.* **4**, 7292; DOI:10.1038/srep07292 (2014).

This work is licensed under a Creative Commons Attribution-NonCommercial-NoDerivs 4.0 International License. The images or other third party material in this article are included in the article's Creative Commons license, unless indicated otherwise in the credit line; if the material is not included under the Creative Commons license, users will need to obtain permission from the license holder in order to reproduce the material. To view a copy of this license, visit http://creativecommons.org/licenses/by-nc-nd/4.0/